Lattice Model for the Adsorption of Benzene in Silicalite I

Chung-Kung Lee and Anthony S. T. Chiang
Dept. of Chemical Engineering, National Central University, Chung-Li, Taiwan, ROC 32054

F. Y. Wu
Dept. of Physics, Northeastern University, Boston, MA 02115

A lattice gas model is used to describe the adsorption of benzene in silicalite I. Using the complete equivalence of the lattice gas with an Ising model and the known exact as well as mean-field results of the latter, we study the thermodynamics of the adsorption and establish criteria on the adsorption energies and site interactions for the existence of a two-phase region. It is shown that a phase change occurs when zigzag paths connecting interacting adsorption sites become energetically favorable. Our model also leads to a sharp rise of the adsorption heat at the transition, albeit at a level less enhanced than experimentally observed.

Introduction

The regularity of the zeolite structure makes it ideal to apply statistical mechanical analysis to its adsorption phenomena. The statistical mechanical approach has been followed by Riekert (1970), Parsonage (1970), Brauer et al. (1970), Woltman and Hartwig (1980), and Ruthven (1984) for adsorptions in zeolites A, X and Y, all containing large cages interconnected by small windows. As a consequence, all these previous investigations have assumed each cage as an independent subsystem. This assumption, however, may not be valid for other types of zeolites, in particular for silicalite.

Silicalite I, first synthesized by Flanigen et al. (1978), is a pure silica zeolite having a structure similar to that of the well-known ZSM-5 zeolite. There are two types of intersecting channels in the structural framework of silicalite I, both defined by ten membered oxygen rings. The channel structure is shown in Figure 1. The first type of the pores comprises small, circular zigzag channels along the a direction with a diameter of about 0.54 nm. The second group includes the larger elliptical straight channels along the b direction with a cross-section of 0.575 × 0.545 nm. For every unit cell (a = 2.002, b = 1.980, and c = 1.336 nm), there are two large pores each 1.980 nm in length (including intersections) and four small pores each 0.66 nm in length. Unlike most other zeolites, silicalite I is hydrophobic in nature and has no exchangeable cation.

Many organic molecules, such as benzene and xylenes, are comparable in sizes to the channels in silicalite I. Due to the strong guest-host interaction under a tight fit, the adsorption of these molecules in silicalite I becomes very unique. Several investigators (Thamm, 1987a,b; Olson et al., 1981; Pope, 1986; Guo et al., 1989; Talu et al., 1989) have reported abnormality in the adsorption of aromatics in silicalite I (or ZSM-5). For instance, the isotherm might change from type I to type IV (Brunauer, 1944) with decreasing temperatures. Furthermore, the adsorption heat was found to rise sharply at some intermediate loading. Several attempts have been made to explain these phenomena qualitatively. These include the description of adsorption as dimer and/or cooperative redistribution of the adsorbed molecules (Thamm, 1987b) and energy heterogeneity of the different channel sections (Stach et al., 1988; Grauert and Fiedler, 1988). Recent works of Guo et al. (1989) and Talu et al. (1989), however, clearly identified the existence of a phase change in the adsorbed phase. To explain their experimental data, they proposed a model that combines a Langmuir and a Hill-de Boer isotherm with a temperature-dependent coefficient. This model, nevertheless, does not take the particular structure of silicalite I into consideration.

It is known that phase change exists in simple lattice gas models with uniform nearest-neighbor interactions (Hill, 1960). Such models, however, always give rise to a type V isotherm, which is convex at the origin. Experimental data of Talu et al., on the other hand, show a clearly concave trend at the origin which changes into a convex curve only at some intermediate loading. Thus, a simple lattice gas model with uniform interactions does not properly describe the adsorption in silicalite I.

Correspondence concerning this article should be addressed to A. S. T. Chiang.

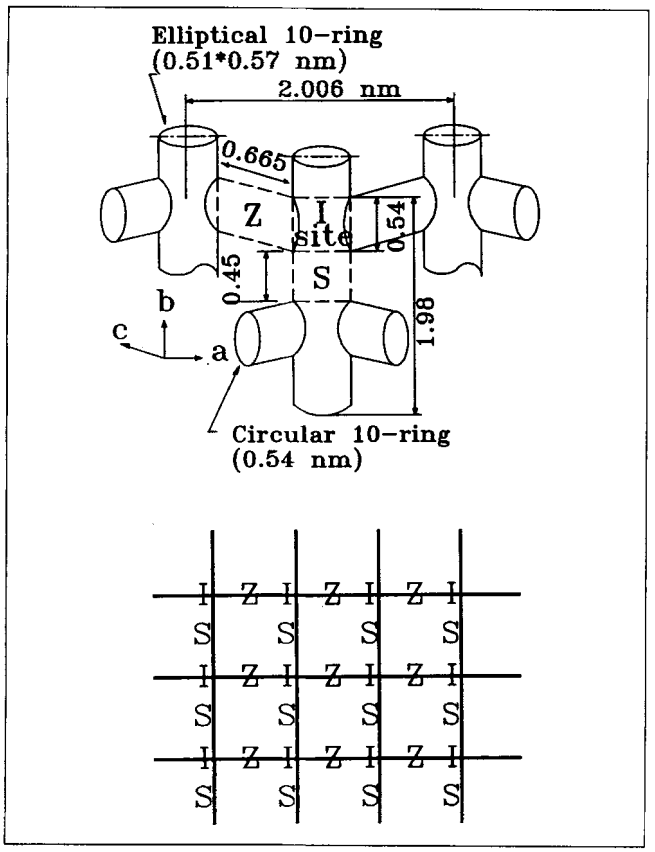

Figure 1. (a) Channel structure of silicalite I; (b) site location in the lattice model.

The molecular dynamic calculation of Reischman et al. (1988) indicated that for the case of *p*-xylene adsorption, there exist three possible adsorption sites of different energies as indicated in Figure 1. Site I, the most favorable, is occupied first. When there are more than four molecules adsorbed per unit cell, site Z will also be occupied. They also found a slightly attractive force between molecules on sites I and Z, as well as between molecules on sites S and Z. But, a strong repulsive force existed between molecules on sites S and I. Monte Carlo simulation works of Grauert and Fiedler (1989) and Talu et al. (1990) also identified three adsorption sites of different energies for benzene in silicalite I. However, the interaction between neighboring molecules was not reported. These facts appear to indicate that a proper modeling of the adsorption of aromatics in silicalite I should include at least three types of adsorption sites with appropriate interactions.

Lattice Gas Model with Three Types of Lattice Sites

We propose to model the adsorption of benzene in silicalite I as a lattice gas on a square lattice with three types of lattice sites, as indicated on Figure 1: S (straight channel), Z (zigzag channel), and I (intersection). The occupation energies for these sites are $-\epsilon_s$, $-\epsilon_z$, and $-\epsilon_i$, respectively. There are four sites of each type in a unit cell, while experimentally only eight molecules of benzene could be adsorbed in a unit cell (Guo et al., 1989; Flanigen et al., 1978; Thamm, 1987a; Wu et al., 1983). Thus, some of these sites must be mutually exclusive. We assume that neighboring S and I sites cannot be simultaneously occupied due to size restriction. The total length from one intersection site to the next is only 0.99 nm. It is too short to accommodate two benzene molecules each about 0.54 nm in size. We further assign interactions $-J_{zi}$ to occupied neighboring Z and I sites. For simplicity, interactions between the S and Z sites are neglected.

Although the modeling is two-dimensional, the structure is similar and the coordination number of each site is the same as that in the silicalite I crystal. Nevertheless, it should be pointed out that the assignment of physical locations is immaterial to the model. The macroscopic results do not change if one interchanges the S, Z, and I subscripts in the following theoretical developments.

For a system with N sites of each type, the grand partition function of the lattice gas can be written as:

$$\Xi(\mu, N, T; J_{zi}, \epsilon_s, \epsilon_z, \epsilon_i) = \sum_{n_s=0,1} \sum_{n_z=0,1} \sum_{n_i=0,1} (\lambda_s)^{\Sigma n_s} (\lambda_z)^{\Sigma n_z} (\lambda_i)^{\Sigma n_i} \prod_{(z,i)} X^{n_z n_i}, \quad (1)$$

where $X = \exp(J_{zi}/kT)$, $\lambda_s = \lambda X_s = \exp[(\mu+\epsilon_s)/kT]$, $\lambda_z = \lambda X_z = \exp[(\mu+\epsilon_z)/kT]$, $\lambda_i = \lambda X_i = \exp[(\mu+\epsilon_i)/kT]$, and the activity $\lambda = \exp(\mu/kT)$. The summation is over all possible occupancies, with $n_i = 1$ (0) denoting the site i being occupied (unoccupied).

This three-site model can be reduced to a nearest-neighbor Ising model (Syozi, 1972). Specifically, we trace over the spin states of Z site replacing it by a single interaction K between I sites. This is done by writing $n = (\sigma + 1)/2$ and

$$\sum_{n_z=0,1} (\lambda_z)^{n_z} X^{n_z(n_1+n_2)} = Fe^{h(\sigma_1+\sigma_2)+K\sigma_1\sigma_2}, \quad (2)$$

or explicitly,

$$1+\lambda_z = Fe^{-2h+K},$$

$$1+\lambda_z X = Fe^{-K},$$

$$1+\lambda_z X^2 = Fe^{2h+K}.$$

Solving for K, h, F, we obtain:

$$e^{4K} = \frac{(1+\lambda_z)(1+\lambda_z X^2)}{(1+\lambda_z X)^2},$$

$$e^{4h} = \frac{1+\lambda_z X^2}{1+\lambda_z},$$

and

$$F^4 = (1+\lambda_z)(1+\lambda_z X)^2(1+\lambda_z X^2). \quad (3)$$

Note that $K > 0$, meaning that the Ising interaction is ferromagnetic.

Similarly for the vertical interactions, we obtain:

$$\sum_{n_s=0,1} (\lambda_s)^{n_s} = Ge^{v(\sigma_1+\sigma_2)+K'\sigma_1\sigma_2}. \quad (4)$$

This results in:

$$e^{4K'} = 1 + \lambda_s,$$

$$e^{4v} = \frac{1}{1+\lambda_s},$$

and

$$G^4 = 1 + \lambda_s. \tag{5}$$

Here, again, $K' > 0$ is ferromagnetic.

In addition, we have:

$$\prod(\lambda_i)^{n_i} = \prod \lambda_i^{(1+\sigma)/2} = \lambda_i^{N/2} \prod(\lambda_i)^{\sigma/2}. \tag{6}$$

Thus, we obtain from Eq. 1, the exact equivalence:

$$\Xi(X, \lambda_s, \lambda_z, \lambda_i) = \lambda_i^{N/2} (FG)^N \Xi_{\text{Ising}} (K, K', H), \tag{7}$$

where Ξ_{Ising} is the partition function of an Ising model with horizontal and vertical interactions K and K', respectively, and a reduced magnetic field H, given by:

$$e^H = \lambda_i^{\frac{1}{2}} e^{2(h+v)}. \tag{8}$$

The occupancy density of each type of sites is:

$$\rho_s = \lambda_s \frac{\partial}{\partial \lambda_s} \left(\frac{\ln \Xi}{N}\right)$$

$$= \frac{\lambda_s}{4}\left(\frac{1}{1+\lambda_s}\right)\frac{\partial f}{\partial K'} - \frac{\lambda_s}{2}\frac{1}{1+\lambda_s}\frac{\partial f}{\partial H} + \frac{\lambda_s}{4}\frac{1}{1+\lambda_s},$$

$$\rho_z = \lambda_z \frac{\partial}{\partial \lambda_z}\left(\frac{\ln \Xi}{N}\right) = \frac{\lambda_z}{4}\left(\frac{1}{1+\lambda_z} - \frac{2X}{1+\lambda_z X} + \frac{X^2}{1+\lambda_z X^2}\right)\frac{\partial f}{\partial K}$$

$$+ \frac{\lambda_z}{2}\left(\frac{X^2}{1+\lambda_z X^2} - \frac{1}{1+\lambda_z}\right)\frac{\partial f}{\partial H}$$

$$+ \frac{\lambda_z}{4}\left(\frac{1}{1+\lambda_z} + \frac{2X}{1+\lambda_z X} + \frac{X^2}{1+\lambda_z X^2}\right),$$

$$\rho_i = \lambda_i \frac{\partial}{\partial \lambda_i}\left(\frac{\ln \Xi}{N}\right) = \frac{1}{2}\left(1 + \frac{\partial f}{\partial H}\right). \tag{9}$$

where

$$f(K, K', H) = \frac{1}{N} \ln \Xi_{\text{Ising}}.$$

The overall occupancy density ρ, which is equal to $(1/3N)(\partial \ln \Xi / \partial \ln \lambda)_{T,N}$, is the average of these three ρ's. We further write (Hill, 1960):

$$kT \ln \Xi = (3N)\phi, \tag{10}$$

$$d(kT \ln \Xi) = SdT + (3N\rho)d\mu + \phi d(3N). \tag{11}$$

The energy U of the lattice gas system is $3N\rho\mu + TS - 3N\phi$. The partial molar energy of the adsorbed molecules $\bar{u}$ is thus:

$$\bar{u} = \frac{1}{3N}\left(\frac{\partial U}{\partial \rho}\right)T, N = \frac{T}{3N}\left(\frac{\partial S}{\partial \rho}\right)T, N + \mu. \tag{12}$$

If there exist two adsorbed phases, the partial molar energy of the system is $(1/3N)(\Delta U/\Delta\rho) = (1/3N)(T\Delta S/\Delta\rho) + \mu$, where ΔS and $\Delta\rho$ are the differences between the two phases. If the gas phase is ideal, the differential heat of adsorption q_d will be $(3/2)RT - \bar{u}$, and the isosteric heat of adsorption q_{st} is $q_d + RT$ (Clark, 1970).

Exact Analysis in the Two-Phase Region

Our lattice gas model has been transformed to an Ising model. In two dimensions, exact solution to the Ising model exists, and for ferromagnetic Ising interactions the phase boundary is $H = 0$ (Onsager, 1944; Chang, 1952; Domb, 1960). For the square lattice, we have:

$$f|_{H=0} = \frac{1}{8\pi^2}\int_0^{2\pi} d\theta \int_0^{2\pi} d\phi \,(\cosh K \cosh K' - \sinh K \cos\theta - \sinh K' \cos\phi), \tag{13}$$

and

$$\frac{\partial}{\partial H} f(K, K', H)|_{H=0\pm} = \pm I_0(K, K'), \tag{14}$$

where

$$I_0(K,K') = [1 - (\sinh 2K)^{-2} (\sinh 2K')^{-2}]^{1/8}. \tag{15}$$

The critical temperature T_c occurs at $I_0 = 0$.

The exact phase envelope of the lattice gas model can now be obtained. For given values of ϵ's and J_{zi}, the equation $H = 0$ can be solved for the activity λ at each temperature. Inserting this activity and the known results of Ising model into the density formula, two densities corresponding to $H = 0\pm$ can be obtained. The trajectory of these densities gives rise to the phase envelope.

For a system to exhibit a phase change, however, there exist constraints for the energies $-\epsilon_s$, $-\epsilon_z$, $-\epsilon_i$, and J_{zi}. For example, the condition $H = 0$ leads to:

$$\lambda^2(X_i X_z X^2 - X_s X_z) + \lambda(X_i - X_s - X_z) - 1 = 0. \tag{16}$$

Since λ is positive, the phase boundary is determined by the positive root of Eq. 16, which turns out to be unique. The necessary condition for the existence of a positive root is $X^2 X_i > X_s$, or equivalently,

$$2J_{zi} + \epsilon_i > \epsilon_s. \tag{17}$$

Another constraint is imposed on the adsorption potential ϕ, also positive by definition. Our numerical results indicate

that ϕ become negative when $2J_{zi}+\epsilon_z+\epsilon_i > 2\epsilon_s$. Combining this inequality with Eq. 17, we obtain the necessary conditions for a solution to exist as:

$$\epsilon_s-\epsilon_z>2J_{zi}+\epsilon_i-\epsilon_s>0. \tag{18}$$

Our numerical results also indicate that sinh $2K$ sinh $2K'$ < 1 when $\epsilon_i > \epsilon_s$. Thus, we regard:

$$\epsilon_s>\epsilon_i. \tag{19}$$

as a third condition for a phase change to occur.

The constraints 18 and 19 do have physical meanings. The conditions $\epsilon_i < \epsilon_s$, $\epsilon_z < \epsilon_s$, and $2J_{zi} + \epsilon_z + \epsilon_i < 2\epsilon_s$ imply that the S sites are the most favorable adsorption sites (as compare to the Z and I sites either individually or as pairs), and the adsorption onto I sites is hindered by nearest-neighbor exclusions. As the pressure is gradually increased, however, some of the Z sites will be occupied, and the filling of the I sites may become more favorable. The constrain $2J_{zi}+\epsilon_i>\epsilon_s$ now comes into play. At some point, the previously adsorbed molecules on S sites will jump to I sites spontaneously.

In addition, the newly occupied I sites will further promote the adsorption of its neighboring Z sites. Thus, many more molecules can be adsorbed onto the partially loaded Z sites without increasing the pressure. This spontaneous jump of molecules from S sites to I sites and the adding of more molecules to Z sites lead to the observed phase change with a discontinuity in occupations.

Finally, the entropy change during the phase change can also be calculated exactly. It is given by:

$$\frac{\Delta S}{k}=N I_0\left\{\frac{\lambda_z \ln \lambda_z}{1+\lambda_z}+\frac{\lambda_s \ln \lambda_s}{1+\lambda_s}-\ln \lambda_i-\frac{\lambda_z X^2 \ln (\lambda_z X^2)}{1+\lambda_z X^2}\right\}. \tag{20}$$

Mean-Field Solution in the Single-Phase Region

Since no exact solution exists for the Ising model outside the phase boundary $H=0$, we use a mean-field analysis to obtain the solution. Following Huang (1987), we write the free energy as:

$$f(K,K',H)=(K+K')m^2+Hm$$

$$-\frac{1+m}{2}\ln\frac{1+m}{2}-\frac{1-m}{2}\ln\frac{1-m}{2}, \tag{21}$$

where m is the solution of:

$$m=\tanh\,[H+2m(K+K')]. \tag{22}$$

It is known that the mean-field solution may not be very accurate near the phase boundary. However, away from the phase boundary, this mean-field solution is a good approximation, and we can use it to obtain the adsorption isotherm as well as the isosteric heat of adsorption in the single-phase region.

The Henry's constant of adsorption can also be derived from the mean-field solution. However, we must first make a translation between the activity and the pressure. The pressure in the gas phase is related to the activity by $P = \lambda\exp(-(\mu_0/kT)$, where the chemical potential μ_0 of the reference state is a function of the temperature. Thus,

$$K=12d_s\lim_{P\to 0}\frac{d\rho}{dP}=12d_s\exp\left(\frac{\mu_0}{kT}\right)\lim_{\lambda=0}\frac{d\rho}{d\lambda}$$

$$=4d_s\exp\left(\frac{\mu_0}{kT}\right)\left\{\exp\left[\frac{\epsilon_s}{kT}\right]\right.$$

$$\left.+\exp\left[\frac{\epsilon_z}{kT}\right]+\exp\left[\frac{\epsilon_z}{kT}\right]\right\}. \tag{23}$$

Here, the density d_s for silicalite I is 0.173×10^{-3} mole of unit cells per gram, and the factor 12 comes from the fact that each unit cell has 12 adsorption sites.

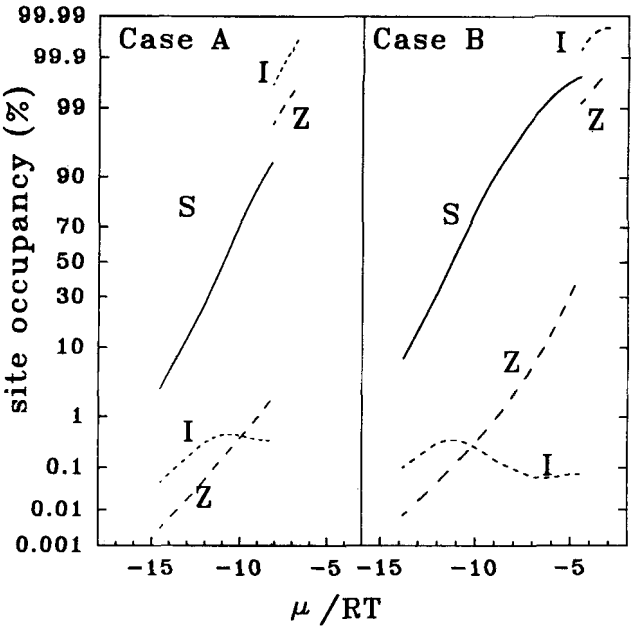

Figure 2. Site occupancy calculated by the mean-field solution with parameter sets A and B.

The sum of the three types of site occupancies is the normalized adsorption isotherm.

Numerical Results

Some typical isotherms are shown in Figures 2 and 3. In these figures, the loading on each type of the sites is drawn on a probability scale. This scale is chosen for two reasons. First of all, minor changes near zero and saturated loadings can be more visible. Secondly, the mean-field solution of a simple noninteracting lattice gas model will be a straight line in this scale, the parameters that used to generate these isotherms are given in Table 1.

As described previously, most of the S sites are filled at very low pressures, corresponding to low chemical potentials. The larger the difference between $\epsilon_i + 2J_{zi}$ and ϵ_s, the lower loading on Z sites is needed to initiate a phase change. This fact can be identified by the difference between the curves of cases A, C and D, and of case B. At the onset of a phase change, all molecules adsorbed on S sites tend to move to I sites. The

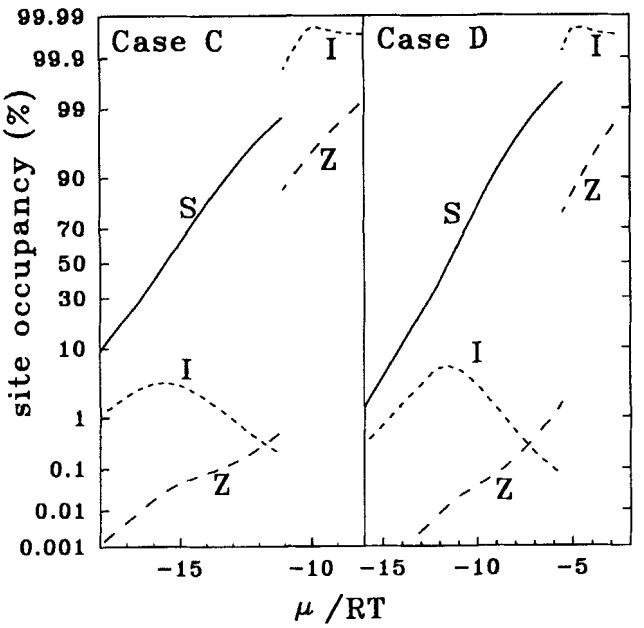

Figure 3. Site occupancy calculated by the mean-field solution with parameter sets C and D.

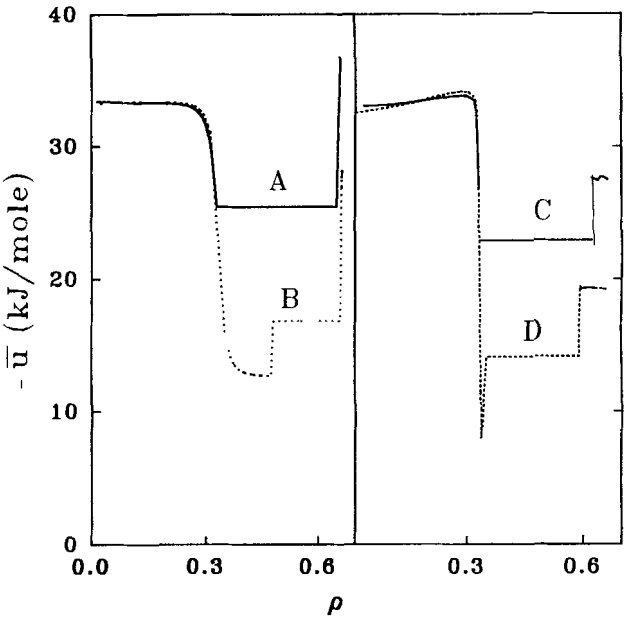

Figure 4. Partial molar internal energy (related to differential heat of adsorption) of the example cases.

The curves were calculated by mean-field solution. The straight lines in the two-phase region are obtained by the exact solution.

loading of S sites drops to nearly zero, which cannot be seen on the scale in these figures. At the same time, the loading S of Z and I sites experience a drastic jump. The amount of Z loading jump depends on the relative magnitudes of $2J_{zi} + \epsilon_z$ and ϵ_i. For small ϵ_i, Z sites are almost saturated after the phase change, as shown in Figure 2; otherwise, free Z sites exist for further adsorption after the phase change.

The general behavior of the partial molar internal energy (differential heat of adsorption) is shown in Figure 4. Since very little adsorption persists after the phase change, the partial molar internal energy of the denser phase occupies only a small fraction in these graphs. Between the two single-phase regions, a constant heat curve computed from the exact solution of the phase boundary is drawn. The discontinuity in the heat curve created by phase change is now apparent.

As indicated by Eq. 23, the initial heat of adsorption is a combination of the occupancy energies of all three types of sites. If ϵ_s is dominant, the adsorption heat will be constant initially, as shown in cases A and B. On the other hand, when the difference between ϵ_i and ϵ_s is much smaller, as in cases C and D, some adsorbed I sites will occur at a low pressure, this leading to a slight upward trend of the heat curve at low loadings as shown in Figure 3.

After all S sites are occupied, further adsorption can occur only on the Z sites. In the case B, for example, where an appreciable adsorption on Z sites occurs before the phase change, the partial molar internal energy drops to exactly ϵ_z as the Z sites are progressively filled. For cases A, C and D, a phase change occurs before an appreciable filling of Z sites. Thus, the partial molar energy is higher than ϵ_z.

The energy change during phase change comes mainly from the trading of the occupation of Z-I sites to S sites. The energies of the two phase are approximately $3N\rho + (2J_{zi} + \epsilon_i + \epsilon_z)/2$ and $3N\rho - \epsilon_s$, respectively. At low temperature, $\rho_+ \approx 2\rho_- \approx 2/3$; thus, we have $(1/3N)(\Delta U/\Delta\rho) \approx 2J_{zi} + \epsilon_i + \epsilon_z - \epsilon_s$, which is always smaller than ϵ_s by the criteria we have found.

In the densely packed phase, most of the I sites are already occupied. Further adsorption occurs only on the few Z sites that are still vacant. Each molecule added would correspond to a release of an energy $2J_{zi} + \epsilon_z$. If this value is higher than ϵ_s, the last molecule adsorbed may evolve more energy than the first molecule adsorbed, as indicated by case A.

Comparison with Experiments

The adsorption heat data observed by Thamm (1987a, b) indicate a constant value of 57.5 kJ/mol for loadings smaller than 4 molecules per unit cell at 300 K. This is followed by a

Table 1. Parameters Used in Numerical Examples

Case	ϵ_s kJ/mol	ϵ_z kJ/mol	ϵ_i kJ/mol	J_{zi} kJ/mol	T_c K	$u_{\text{phase change}}$ kJ/mol
A*	33.4724	12.552	20.920	12.552	553.6846	-25.593
	$\epsilon_i > \epsilon_z$, $2J_{zi} + \epsilon_z > \epsilon_s > \epsilon_i$					
B*	33.472	12.552	20.920	7.5312	534.7021	-16.8
	$\epsilon_i > \epsilon_z$, $\epsilon_s > 2J_{zi} + \epsilon_z > \epsilon_i$					
C*	33.472	12.552	29.288	7.5312	384.1924	-22.948
	$\epsilon_i > \epsilon_z$, $\epsilon_s > \epsilon_i > 2J_{zi} + \epsilon_z$					
D*	33.472	4.184	29.288	7.5312	513.3525	-14.111
	$\epsilon_i > \epsilon_z$, $\epsilon_s > \epsilon_i > 2J_{zi} + \epsilon_z$					

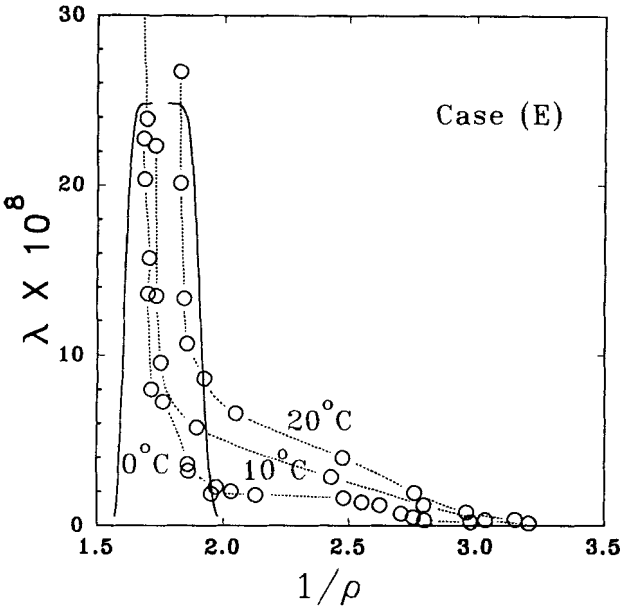

Figure 5. Comparison of the experimental isotherms (Guo et al. 1989) to the phase boundary (solid line) of the present model using parameter set E.

slight drop to 48 kJ/mol, and then a sharp rise to 65 kJ/mol. At near saturation loading, the adsorption heat reaches 75 kJ/mol.

Based on the previous discussion, we assume ϵ_s = 51 kJ/mol, ϵ_z = 41 kJ/mol and J_{zi} = 15 kJ/mol. The sharp rise at intermediate loading is the result of heat evolved during the phase change, which we know is equal to $2J_{zi} + \epsilon_z + \epsilon_i - \epsilon_s$ at low temperature. It, however, was not possible to solve for the unknown ϵ_i from the data given.

Further information has been given by Talu et al. (1989). Their study indicates that the critical temperature of benzene adsorbed on silicalite I is 311 K. However, the initial heat of adsorption they found is 70 kJ/mol, and isotherms measured at four different temperatures were also listed.

Taking the three energies read from Thamm's data and adopting the critical temperature given by Talu et al., we are left with no adjustable parameter, and a value of 22.11567 kJ/mol is found for ϵ_i. The phase boundary calculated with these constants is assigned the case E and is compared with the isotherm data of Talu et al. in Figure 5. Because the data were given as a function of the pressure, the reference state chemical potential μ_0 can be obtained by matching the scales. In particular, the points immediately before and after the phase change are matched to the phase boundary by moving the ln(P) axis. The reference state so obtained also enables us to compute the Henry's law constants. The results are given in Table 2.

The comparison in Figure 5 is not very satisfactory, since the phase boundary predicts a much more compact packing than observed. Most of the phase changes observed were located around 4 molecules/unit cell [ρ = (1/3) as compared to the predicted phase change at 6 molecules/unit cell [ρ =

Table 2. Parameters Used for Comparisons with Experimental Data

Case	ϵ_s kJ/mol	ϵ_z kJ/mol	ϵ_i kJ/mol	J_{zi} kJ/mol	
E	51	41	22.11567	15	
	Test Temp.	$\exp\left(\frac{\mu_0}{RT}\right)$	μ_0	$K \times RT$	$\bar{u}_{\text{phase change}}$
	K	*	m³/mol	m³/kg	kJ/mol
	273	1.5831×10^{-10}	-5.1222×10^4	1.4482×10^3	−44.044
	283	9.1089×10^{-12}	-5.9817×10^4	3.9127×10^1	−44.15
	293	4.9559×10^{-12}	-6.3413×10^4	1.0541×10^1	−44.258
Case	ϵ_s kJ/mol	ϵ_z kJ/mol	ϵ_i kJ/mol	J_{zi} kJ/mol	
F	51	35.72839	47.51891	2.974541	
	Test Temp.	$\exp\left(\frac{\mu_0}{RT}\right)$	μ_0	$K \times RT$	$\bar{u}_{\text{phase change}}$
	K	*	m³/mol	m³/kg	kJ/mol
	273	7.7316×10^{-10}	-4.7622×10^4	8.5084×10^3	−38.588
	283	5.3568×10^{-11}	-5.5648×10^4	2.7902×10^2	−38.613
	293	2.8856×10^{-11}	-5.9121×10^4	7.4994×10^1	−38.642
	303	1.5829×10^{-11}	-6.2652×10^4	2.1523×10^1	−38.673
Case	ϵ_s kJ/mol	ϵ_z kJ/mol	ϵ_i kJ/mol	J_{zi} kJ/mol	
G	51	41.09647	40.95839	6.708110	
	Test Temp.	$\exp\left(\frac{\mu_0}{RT}\right)$	μ_0	$K \times RT$	$\bar{u}_{\text{phase change}}$
	K	*	m³/mol	m³/kg	kJ/mol
	273	5.4804×10^{-11}	-5.363×10^4	5.0821×10^2	−45.675
	283	4.2435×10^{-12}	-6.1614×10^4	1.8514×10^1	−45.76
	293	2.5375×10^{-12}	-6.5044×10^4	5.4933×10^0	−45.844
	303	1.5356×10^{-12}	-6.8529×10^4	1.7307×10^0	−45.929

*Taking unit pressure in pascal as reference pressure.

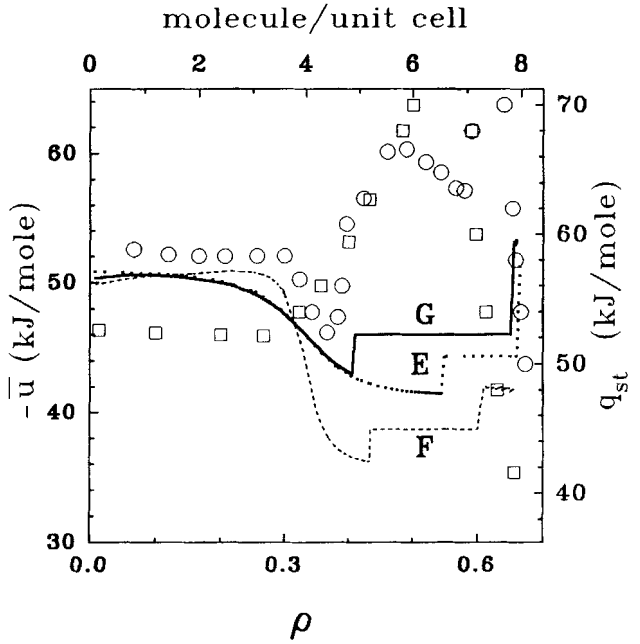

Figure 6. Experimental adsorption heat (Thamm, 1987a; Pope, 1986) vs. calculation from the present model using different parameter sets.

1/2). Furthermore, the adsorption heat drops much earlier than that indicated by experimental data shown in Figure 6. Considering the combination of data from two different sources and the use of a rough estimation to the site energies, the difference is not unexpected.

We have tried to use other sets of parameters in Table 2. With these parameter sets, the phase boundary calculated by the exact solution matched the experimental isotherm much better, as shown in Figures 7 and 8. Case F, which gives a better match and predicts a Henry's law constant of 7.5 × 10^1 m^3/kg at 30°C as compared to the observed value of 1.25

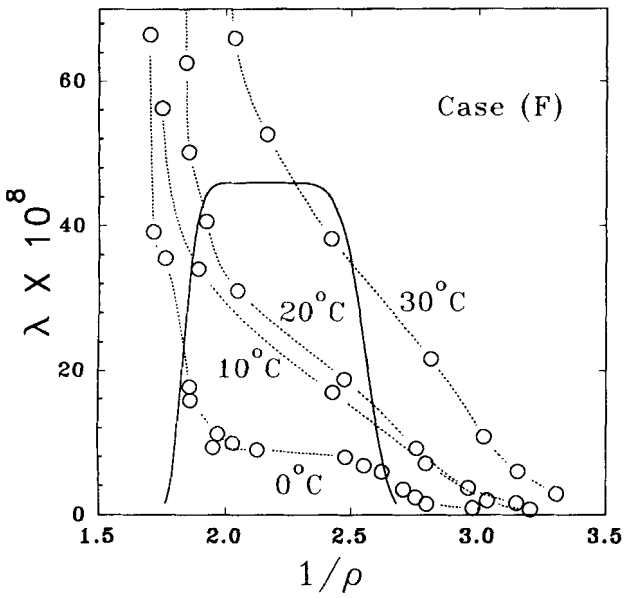

Figure 7. Experimental isotherms vs. phase boundary (solid line) of the present model using parameter set F.

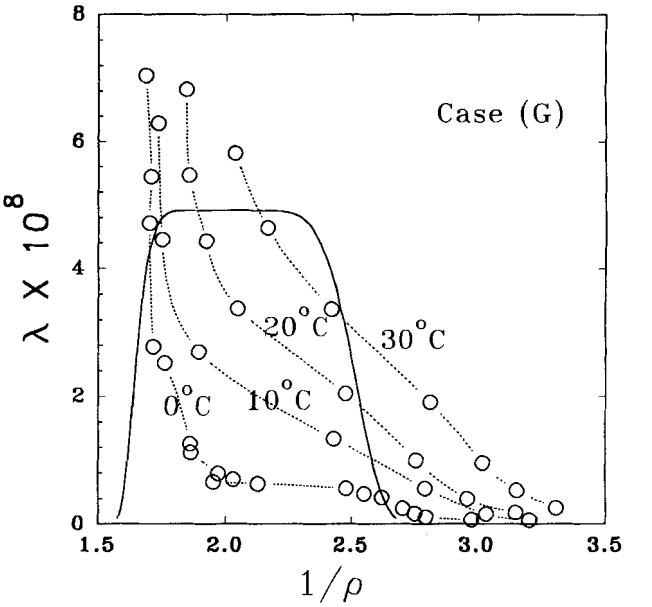

Figure 8. Experimental isotherms vs. phase boundary (solid line) of the present model using parameter set G.

× 10^2 m^3/kg (Talu et al., 1991). The adsorption heat, however, does not improve appreciably.

It seems that it is intrinsic that our model does not lead to a rise of differential adsorption heat over its initial value ϵ_s. To have a larger energy jump at phase transition, the interaction energy between molecules on Z and I sites must be larger in the second phase than in the first phase. This is so because an array of molecules is formed in the second phase, occupying alternating S and I sites. For example, molecules in the channels may have several favorable orientations depending on its neighboring occupations. The site energy as well as the binary molecule interaction should be averaged over these orientations.

Stach et al. (1988) have used a cell model to explain Thamm's data of the heat of adsorption. They assumed the existence of some perturbed intersection site I', in addition to the three types of sites. By fitting to experimental data, a series of energies were calculated for different occupancy levels. Upon some drastic and uncontrolled simplifications, they arrived at a qualitative prediction of the adsorption heat. However, they were unable to generate a satisfactory phase diagram. Our model, however crude it might be, is able to point out pertinent phenomena associated with the phase change.

It is now clear that a proper lattice model to describe the adsorption of benzene in silicalite I should include three different types of sites with attractive and repulsive interactions between Z-I and S-I pairs of molecules, respectively. For molecules such as *p*-xylene, where an increasing heat of adsorption at low loadings was found, an additional attractive interaction between Z-S pairs may be needed. However, the solution of such a model can be obtained only by numerical techniques.

Conclusions

We have demonstrated that with a simple lattice model having three types of lattice sites, some important characteristics of the adsorption in silicalite I can be described. In particular, the step changes in isotherms and heat curves are found to

correspond to the re-arrangement of adsorbed molecules to a denser packing state, in which benzene molecules form a long chain along the zigzag a, c axis.

Acknowledgment

Two of us (CKL and ASTC) have been supported by NSC of ROC through the grant NSC-80-0402-E008-05; the work of FYW has been supported by National Science Foundation Grants INT-8902033 and DMR-9015489.

Notation

f = $(1/N) \ln \Xi_{\text{Ising}}$
F = scaling factor for horizontal interaction transformation
$f|_{H=0}$ = exact solution of the Ising model at the phase boundary
G = scaling factor for vertical interaction transformation
h = magnetic strength of the Ising model from the horizontal interaction
H = reduced magnetic field of Ising model
I = adsorption site of interaction channel section
I_0 = spontaneous magnetization of Ising model
J_{zi} = interaction between the neighboring occupied Z and I sites
K = Henry's constant, mol/kg·pa
K = horizontal interaction of the square Ising model
K' = vertical interaction of the square Ising model
k = Boltzmann constant
m = magnetization per site of Ising model
n = occupancy number of S, Z and I sites (n = 0, 1)
n_i = occupancy number of I sites
n_s = occupancy number of S sites
n_z = occupancy number of Z sites
N = total number of each type adsorption sites
P = vapor pressure
q_{st} = isosteric heat of adsorption, kJ/mol
q^{∞} = number of all different sites per weight of silicalite, 2.076 mol/kg
R = gas constant
S = adsorption site of straight channel section
ΔS = entropy change during phase change
T = temperature, K
T_c = critical temperature, K
U = energy of lattice gas system
ΔU = energy change during phase change
$\bar{u}_{\text{phase change}}$ = partial molar internal energy during phase change
v = magnetic strength of the Ising model from the vertical interaction
V = system volume or number of adsorption sites
X = exp (J_{zi}/kT)
X_i = exp (ϵ_i/kT)
X_s = exp (ϵ_s/kT)
X_z = exp (ϵ_z/kT)
Z = adsorption sites of zigzag channel section

Greek letters

Ξ_{Ising} = partition function of Ising model with horizontal K and vertical K' interactions
ϵ_i = occupation energy of I sites, kJ/mol
ϵ_s = occupation energy of S sites, kJ/mol
ϵ_z = occupation energy of Z sites, kJ/mol
λ = absolute activity
λ_i = λX_i
λ_s = λX_s
λ_z = λX_z
σ = spin variables of Ising model, + 1 or − 1
Ξ = grand partition function of system with $3N$ sites
μ = chemical potential
μ_0 = reference state chemical potential
ρ = overall occupancy density
$\Delta\rho$ = occupancy density change during phase change
ρ_i = occupancy density of I sites
ρ_s = occupancy density of S sites
ρ_z = occupancy density of Z sites
ρ_+, ρ_- = occupancy density corresponding to $H = 0\pm$
ϕ = adsorption potential per unit cell

Subscripts

i,s,z = interaction, straight channel, zig-zag channel adsorption sites

Literature Cited

Brauer, P., A. A. Lopatkin, and G. Ph. Stepanez, "Calculation of Some Adsorption Properties of Zeolites by Statistical Methods," *Adv. Chem. Ser.*, **102**, 97 (1970).

Brunauer, S., *The Adsorption of Gases and Vapors*, Oxford Univ. Press, London (1944).

Chang, C. H., "The Spontaneous Magnetization of a Two-Dimensional Rectangular Ising Model," *Phys. Rev.*, **88**, 1422 (1952).

Clark, A., *Theory of Adsorption and Catalysis*, Academic Press, New York (1970).

Domb, C., "On the Theory of Cooperative Phenomena in Crystals," *Adv. Phys.*, **9**, 149 (1960).

Flanigen, E. M., J. M. Bennett, R. W. Grose, J. P. Cohen, R. L. Patten, R. M. Kirchner, and J. V. Smith," Silicalite, A New Hydrophobic Crystalline Silica Molecular Sieve," *Nature*, **271**, 512 (1978).

Grauert, B., and K. Fiedler, "Monte Carlo Calculations: Thermodynamic Functions in Zeolites II. Adsorption of Benzene on Silicalite," *Adsorp. Sci. Technol.*, **5**, 191 (1988).

Guo, C. J., O. Talu, and D. T. Hayhurst, "Phase Transition and Structural Heterogeneity: Benzene Adsorption on Silicalite," *AIChE J.*, **35**, 573 (1989).

Hill, T. L., *Introduction to Statistical Thermodynamics*, Addison Wesley, MA (1960).

Huang, K., *Statistical Mechanics*, Wiley, New York (1987).

Olson, D. H., G. T. Kokotallo, S. L. Lawton, and M. W. Meler, "Crystal Structure and Structure-Related Properties of ZSM-5," *J. Phys. Chem.*, **85**, 2238 (1981).

Onsager, L., "Crystal Statistics: I. a Two-Dimensional Model with an Order-Disorder Transition," *Phys. Rev.*, **65**, 117 (1944).

Parsonage, N. G., "Effect of Repulsions Between Sorbed Molecules on the Sosteric Heats of Substances Sorbed in Zeolites: A Simple Theory," *Trans. Farad. Soc.*, **66**, 723 (1970).

Pope, C. G., "Sorption of Benzene, Toluene, and P-Xylene on Silicalite and H-ZSM-5," *J. Phys. Chem.*, **90**, 835 (1986).

Reischman, P. T., K. D. Schmitt, and D. H. Olson, "A Theoretical and NMR Study of P-Xylene Sorption into ZSM-5," *J. Phys. Chem.*, **92**, 5165 (1988).

Riekert, L., "Sorption, Diffusion, and Catalytic Reaction in Zeolites," *Adv. Catal.*, **21**, 287 (1970).

Ruthven, D. M., *Principles of Adsorption & Adsorption Processes*, Wiley, New York (1984).

Stach, H., R. Wendt, K. Fiedler, B. Grauret, J. Janchen, and H. Spindler, *Characterization of Porous Solids*, K. K. Unger et al., eds., Elsevier, Amsterdam (1988).

Syozi, I., *Phase Transition and Critical Phenomena*, Vol. 1, C. Domb and M. S. Green, eds., Academic Press, New York (1972).

Talu, O., C. J. Guo, and D. T. Hayhurst, "Heterogeneous Adsorption Equilibria with Comparable Molecule and Pore Sizes," *J. Phys. Chem.*, **93**, 7294 (1989).

Talu, O., "Behavior of Aromatic Molecules in Silicalite by Direct Integration of Configurational Integral," *AIChE Meeting*, Chicago (1990).

Thamm, H., "Adsorption Site Heterogeneity in Silicalite: a Calorimetric Study," *Zeolites*, **7**, 341 (1987a).

Thamm, H., "Calorimetric Study on the State of Aromatic Molecules Sorbed on Silicalite," *J. Phys. Chem.*, **91**, 8 (1987b).

Woltman, A. W., and W. H. Hartwig, "The Solution Theory Modeling of Gas Adsorption on Zeolites," *ACS Symp. Ser.*, **135**, 3 (1980).

Wu, P., A. Debebe, and Y. H. Ma, "Adsorption and Diffusion of C_6 and C_8 Hydrocarbons in Silicalite," *Zeolites*, **3**, 118 (1983).

Manuscript received June 7, 1991, and revision received Nov. 14, 1991.